2276 *Chem. Mater.* **2010,** *22,* 2276–2286
DOI:10.1021/cm903095q

CHEMISTRY OF MATERIALS
Article

Diasteroselective Structure Directing Effect of (1*S*,2*S*)-2-Hydroxymethyl-1-benzyl-1-methylpyrrolidinium in the Synthesis of ZSM-12

Raquel García,*[,†] Luis Gómez-Hortigüela,[†,‡] Félix Sánchez,[§] and Joaquín Pérez-Pariente[†]

[†]*Instituto de Catálisis y Petroleoquímica* (*CSIC*), *C/Marie Curie 2, 28049 Cantoblanco, Madrid, Spain,* [‡]*Department of Chemistry, Third Floor, Kathleen Lonsdale Building, University College London, Gower Street, WC1E 6BT, London, United Kingdom, and* [§]*Instituto de Química Orgánica General* (*CSIC*), *C/Juan de la Cierva, 3, 28006, Madrid, Spain*

Received October 6, 2009. Revised Manuscript Received February 8, 2010

The chiral cation (1*S*,2*S*)-2-hydroxymethyl-1-benzyl-1-methylpyrrolidinium (bmpm) and a 50% mixture of this with its diastereoisomer (1*R*,2*S*)-2-hydroxymethyl-1-benzyl-1-methylpyrrolidinium have been prepared and tested as structure directing agents (SDAs) in the synthesis of pure-silica zeolites in fluoride medium. The S,S isomer has been shown to efficiently direct the crystallization of zeolite ZSM-12 (MTW); in contrast, the use of a mixture of the two diastereoisomers as a SDA does not lead to the formation of the ZSM-12 structure under the same synthesis conditions, thus suggesting a lower efficiency of the R,S isomer to direct the crystallization of the structure. A computational study based on molecular mechanic simulations allowed explanation of the efficient structure directing role of the S,S isomer in terms of a high host−guest interaction due to a strong structural relationship between the MTW topology and the molecular geometry of the S,S isomer. However, the simulations revealed that the interaction developed by the R,S diasteroisomer with the MTW framework is smaller due to a worse fitting of its molecular structure with the zeolite topology, providing an explanation for the experimental observations.

Introduction

Nowadays, there is an increasing demand for enantiomerically pure compounds in the pharmaceuticals and fine chemicals industries which prompts a strong interest in processes able to differentiate chiral enantiomers, such as the resolution of racemic mixtures and asymmetric synthesis reactions. The design of solid sorbents and heterogeneous catalysts with combined shape selectivity and enantioselectivity represents a particularly attractive option, where microporous materials (including zeolites and zeotypes) are excellent candidates to achieve this goal. Zeolites are a class of crystalline microporous molecular sieves whose network is comprised of corner-sharing SiO_4 and AlO_4 tetrahedral units, giving place to a periodic three-dimensional microporous framework. The structure of these materials is comprised of pores and cavities of molecular dimensions, which together with their wide structural and compositional chemistry and their stability provides a range of potential applications to these materials, which are used as shape selective catalysts, adsorbents, and ion exchangers.[1,2] In this context, chirality is one of the most desirable properties for a zeolite structure since the constrained geometry of its framework could eventually control the stereoselectivity of chiral catalytic reactions or result in enantioselective sorption or separation processes, therefore allowing for obtaining optically pure chiral products.[3]

Several approaches have been attempted to introduce chirality in zeolite materials. The most promising approach to date is the immobilization of homogeneous chiral catalysts inside the inorganic solid matrix,[4] thus easing the processes of separation, handling, and recovery of the chiral catalysts. Some enantioselectivity has also been achieved by anchoring chiral modifiers to the microporous materials, in the vicinity of the active sites.[5] In these cases, the zeolitic host might also give additional selectivity by molecular sieving effects.[6] However, in both cases the chiral information is contained in the molecular component attached to an otherwise achiral solid. A more interesting approach comes from the synthesis of an intrinsically chiral framework, in which chirality is imprinted in the inorganic solid. Among the known zeolite structures, only a few of them are known to contain chiral channels,[7] though in a recent paper 20 more zeolite structures have been recognized as possessing chiral networks;[8] indeed,

*Corresponding author. Phone: + 34 91 5854796. E-mail: rgs@icp.csic.es.

(1) Davis, M. E. *Nature* **2002**, *417*, 813.
(2) Corma, A. *J. Catal.* **2003**, *216*, 298.
(3) Davis, M. E. *Top. Catal.* **2003**, *25*, 3.
(4) Mc Morn P.; Hutchings, G. J. Chem. Soc. Rev., **2004**, *33*, 108, and references therein.
(5) Davis, M. E. Microporous Mesoporous Mater., **1998**, *21*, 173, and references therein.
(6) Bedioui, F. *Coord. Chem. Rev.* **1995**, *144*, 39.
(7) Yu, J.; Xu, R. *J. Mater. Chem.* **2008**, *18*, 4021.
(8) Dryzun, C.; Mastai, Y.; Shvalb, A.; Avnir, D. *J. Mater. Chem.* **2009**, *19*, 2062.

 Published on Web 03/04/2010

in this work the authors demonstrated that chiral zeolites are actually able to perform enantioselective operations. Very recently, a new chiral zeolite topology has been discovered.[9]

Zeolite beta is the commonly cited example of a chiral zeolite structure. This zeolite is a heavily intergrown material constituted of at least three closely related structures, polymorphs A, B, and C. Polymorph A is in the form of two enantiomorphs containing a helical pore along the *c*-axis,[10] while polymorphs B and C do not show chirality. In recent years, polymorphs B and C have been synthesized as pure phases,[11,12] but to date, it has not been possible to obtain polymorph A as a pure phase. It was reported that a zeolite beta enriched in polymorph A was obtained by using a chiral SDA, and this sample of zeolite beta was capable of performing enantioselective adsorption and catalysis, yielding a low enantiomeric excess.[13]

The hydrothermal synthesis of zeolite materials often requires the presence of organic molecules, usually called structure directing agents (SDAs), which organize the inorganic tetrahedral units into a particular topology around themselves, therefore providing the initial building blocks for further crystallization of a particular structure type.[14] These organic molecules are encapsulated within the void space of the nascent frameworks, thus keeping occluded after the crystallization process. Hence the size and shape of the SDA plays an important role in determining the outcome of zeolite syntheses; actually, there is usually some correlation between the shape of the molecule and that of the pores crystallized in its presence.[15] In this context, the main strategy traditionally followed to synthesize a chiral zeolite framework is the use of an asymmetric organic molecule as a structure directing agent to impart chirality into the inorganic framework. For a transfer of the chirality from the SDA molecule to the inorganic framework to occur, a close structural relationship between the host and the guest species should exist. In this regard, it is worth mentioning that, in some cases, the structure directing effect of organic molecules in the synthesis of zeolite materials is so strong that different isomers of the same organic molecule can show different phase selectivities. Some examples of this behavior are the different structure directing effect that exert the diastereoisomers of the cation 4,4′-trimethylenebis(1-benzyl-1-methylpiperidinium) on the synthesis of zeolite beta;[16] the specificity of the trans isomer of *N*,*N*-diethyl-2-methyldecahydroquinolinium in the synthesis of SSZ-56;[17] the polycyclic SDA used in the synthesis of zeolite SSZ-73 (SAS);[18] or the cis and trans isomers of *N*,*N*-diethyldecahydroquinolinium, which direct the crystallization of several different zeolite structures for each of them.[19]

Recent work in our group has demonstrated the efficient structure directing role of (*S*)-*N*-benzyl-2-pyrrolidinemethanol in the synthesis of AFI-type microporous aluminophosphates.[20,21] In these works, we observed that the use of this molecule as a SDA provides a rich supramolecular chemistry that can enhance its molecular chiral nature and thus the eventual transfer of the chirality to the microporous framework. On the basis of these grounds, we have studied in this work the structure directing effect of a related molecule, 2-hydroxymethyl-1-benzyl-1-methylpyrrolidinium (bmpm), in the synthesis of all-silica zeolites. In this case, the attachment of a methyl group to the tertiary amine provides a more rigid asymmetric atom in the SDA molecule, what could eventually enhance the chiral character of the SDA, favoring in principle the transfer of chirality to the framework. Besides, the presence of two rings (phenyl and pyrrolidine) provides to this molecule a high rigidity, a feature that is also required for a transfer of the chirality to the nascent framework, provided a strong structure directing effect occurs. In this work we report the results we have obtained using the S,S diasteroisomer alone as well as a mixture of the S,S and R,S diastereisomers of the chiral cation bmpm as SDA. The synthesis and characterization of the materials are complemented with a molecular modeling study aimed to understand the different structure directing efficiency of the S,S and R,S diasteroisomers for the synthesis of the zeolite. A secondary aim of this study is to experimentally validate the theoretical predictions provided by the computational simulations by using a single diasteroisomer and a mixture of both diastereoisomers in the synthesis of the zeolite.

Experimental Section

Synthesis of SDA Cation. Both the pure S,S diastereoisomer and the mixture of R,S and S,S diastereoisomers were prepared according to Figure 1. As shown in this figure, the different products are obtained depending on the initial tertiary amine, making use of the different steric constraint provided by the methyl or benzyl groups.

To prepare the pure *S*,*S* bmpm diastereoisomer (route 1), the starting amine (*S*)-1-benzyl-2-pyrrolidinemethanol was methylated in order to obtain the quaternary ammonium cation, (1*S*,2*S*)-2-hydroxymethyl-1-benzyl-1-methylpyrrolidinium (bmpm) iodide. In a typical preparation, 50.0 g of (*S*)-1-benzyl-2-pyrrolidinemethanol (Aldrich, 97%) were added over a solution of 55.66 g of CH_3I (50% exc., Fluka) in ethanol. After stirring

(9) Sun, J.; Bonneau, C.; Cantín, A.; Corma, A.; Díaz-Cabañas, M. J.; Moliner, M.; Zhang, D.; Li, M.; Zhou, X. *Nature* **2009**, *458*, 1154.
(10) Treacy, M. M. J.; Newsam, J. M. *Nature* **1988**, *332*, 249.
(11) Corma, A.; Moliner, M.; Cantin, A.; Díaz-Cabañas, M. J.; Jorda, J. L.; Zhang, D.; Sun, J.; Jansson, K.; Hovmöller, S.; Zou, X. *Chem. Mater.* **2008**, *20*, 3218.
(12) Cantin, A.; Corma, A.; Díaz-Cabañas, M. J.; Jorda, J. L.; Moliner, M.; Rey, F. *Angew. Chem., Int. Ed.* **2006**, *45*, 8013.
(13) Davis, M. E.; Lobo, R. F. *Chem. Mater.* **1992**, *4*, 756.
(14) Cundy, C. S.; Cox, P. A. *Chem. Rev.* **2003**, *103*, 663.
(15) Gies, H.; Marler, B. *Zeolites* **1992**, *12*, 42.
(16) Tsuji, K.; Beck, L. W.; Davis, M. E. *Microporous Mesoporous Mater.* **1999**, *28*, 519.
(17) Elomari, S.; Burton, A.; Medrud, R. C.; Grosse-Kunstleve, R. *Microporous Mesoporous Mater.* **2009**, *118*, 325.
(18) Kim, C.; Hwang, S.-J.; Burton, A. W.; Zones, S. I. *Microporous Mesoporous Mater.* **2008**, *116*, 227.
(19) Lee, G. S.; Nakagawa, Y.; Hwang, S.-J.; Davis, M. E.; Wagner, P.; Beck, L.; Zones, S. I. *J. Am. Chem. Soc.* **2002**, *124*, 7024.
(20) Gómez-Hortigüela, L.; Corà, F.; Catlow, C. R. A.; Pérez-Pariente, J. *Phys. Chem. Chem. Phys.* **2006**, *8*, 486.
(21) Gómez-Hortigüela, L.; Blasco, T.; Pérez-Pariente, J. *Microporous Mesoporous Mater.* **2007**, *100*, 55.

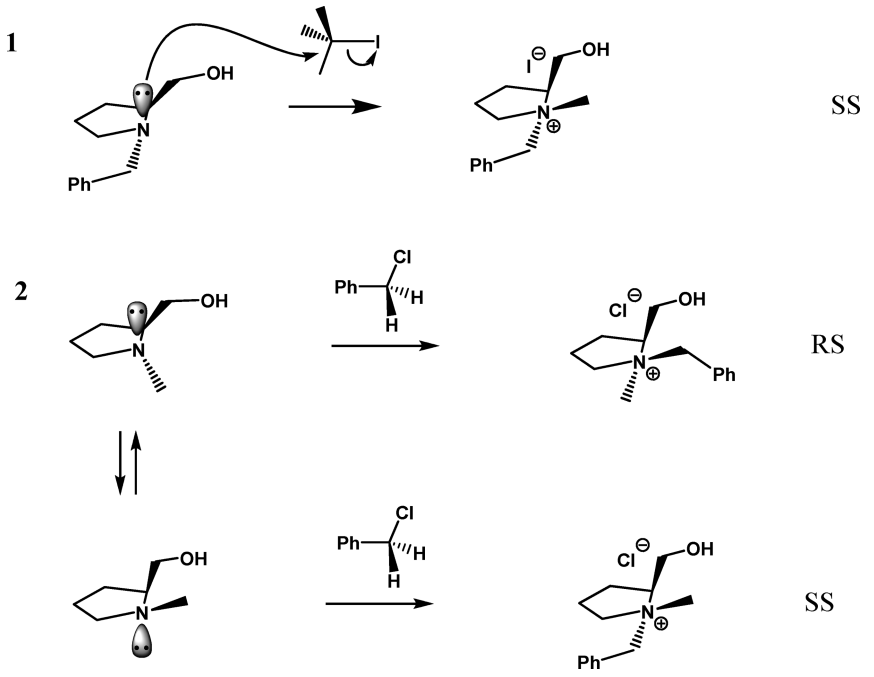

Figure 1. Schematic view of the two attacks that take place in the synthesis of (1) the pure S,S diasteroisomer (route 1, top) and (2) the mixture of diasteroisomers (route 2, bottom), showing the diasteroisomers that are formed depending on the initial reactant used.

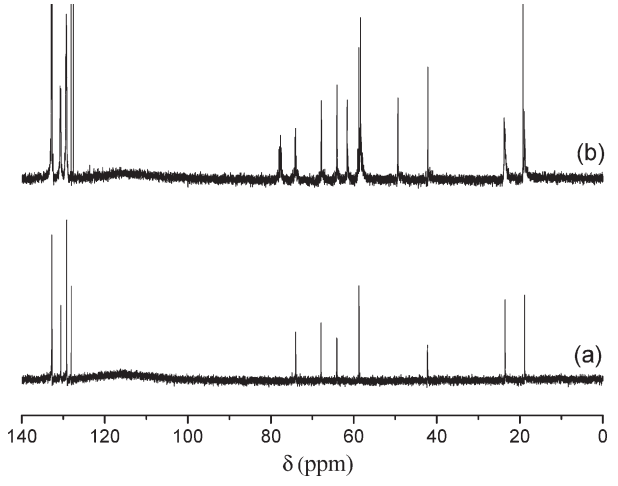

Figure 2. ^{13}C NMR spectrum of the product from synthesis route 1, the iodide salt of the pure *S*,*S*-bmpm (a) or route 2, the chloride salt of the mixture of diastereoisomers SS and RS of bmpm (b).

for 5 days at room temperature, the ethanol was removed under vacuum at 60 °C. The final solid product (~81% yield) was exhaustively washed with diethyl ether, recrystallized from acetone (mp 143−144 °C), and characterized by ^{13}C and ^{1}H nuclear magnetic resonance (NMR) (Figure 2) and chemical CHN analysis. (Calculated for $C_{13}H_{20}NOI$: C = 46.8, H = 6, N = 4.2. Found: C = 47.1, H = 5.9, N = 4.3).

A mixture of the S,S and R,S diastereoisomers was prepared according to route 2 by benzylation of (*S*)-1-methyl-2-pyrrolidinemethanol. A total of 13.02 g of (*S*)-1-methyl-2-pyrrolidinemethanol (96%, Aldrich) was added over a solution of 20.57 g (50% exc.) of benzylchloride (99%, Aldrich) in ethanol. After 24 h of stirring at room temperature, the ethanol was removed under vacuum to yield the final solid product (~89% yield). The solid was exhaustively washed with diethyl ether, dried, and characterized by ^{13}C NMR and chemical CHN analysis. (Calculated for $C_{13}H_{20}NOCl$: C = 64.6, H = 8.3, N = 5.8. Found: C = 63.7, H = 8.3, N = 5.7).

The amount of each isomer was determined from the integral measures of the ^{1}H NMR spectrum of the iodide salt of the mixture of isomers (see the Supporting Information). The iodide form of the mixture of isomers was obtained by stirring an equimolecular amount of the chloride salt previously synthesized and potassium iodide (Aldrich) in acetone. The potassium chloride is separated by filtration, and the acetone is evaporated to yield the final solid product quantitatively.

The hydroxide forms of the quaternary ammonium salts, (1*S*,2*S*)-2-hydroxymethyl-1-benzyl-1-methylpyrrolidinium (bmpm) iodide, and the mixture of (1*S*,2*S*)- and (1*R*,2*S*)-2-hydroxymethyl-1-benzyl-1-methylpyrrolidinium (bmpm) chloride were obtained by ion exchange with an anionic resin (Amberlite IRN-78; exchange capacity, 4 meq/g; Supelco). The hydroxide concentration of the SDA solution was determined by titration with a 0.05 M HCl solution (Panreac) using phenolphthalein (Aldrich) as an indicator.

Zeolite Synthesis. The S,S pure bmpm isomer or the mixture of isomers were employed as SDAs in pure silica preparations in fluoride medium. In a typical experiment, 9.79 g of tetraethylorthosilicate (TEOS, Aldrich, 98%) were hydrolyzed over 15.41 g of the hydroxide aqueous solution (36%) of the SDA. The mixture was stirred until the excess of water over that required to reach the desired composition was evaporated, and then 1.04 g of HF (Panreac, 48%) was added and mixed to create a homogeneous gel of composition 0.54 bmpmOH/0.54 HF/1 SiO_2/4.7 H_2O. The gel was introduced into 20 mL Teflon-lined stainless steel autoclaves, which were heated statically under autogenous pressure for selected periods of time (Table 1). The solid products were recovered by filtration, washed with water and ethanol, and dried at room temperature overnight. Selected samples were calcined at 550 °C under a continuous flow of N_2 (100 mL/min) for 1 h followed by air (100 mL/min) for 6 h in order to remove the occluded organic material.

Characterization. Powder X-ray diffraction (XRD) patterns were recorded on a Panalytical X'Pro diffractometer using Cu K_α radiation. Thermogravimetric analyses (TGA) were carried out on a Perkin-Elmer TGA7 instrument. The samples were

Table 1. Syntheses Conditions and Products of Hydrothermal Synthesis Performed with the Pure SS bmpm Isomer and the Mixture of the RS and SS Isomers, For a Gel Composition of 0.54 bmpmOH/0.54 HF/ 1 SiO_2/4.7 H_2O

gel	T (°C)	t (days)	product
SS-150-25	150	25	ZSM-12
SS-150-37	150	37	ZSM-12
SS-135-25	135	25	ZSM-12
SS-135-37	135	37	ZSM-12
SS-135-6	135	6	A[a]
SS-135-12	135	12	ZSM-12+A
SS-135-16	135	16	ZSM-12
SS-135-26	135	26	ZSM-12
RSSS-135-13	135	13	A
RSSS-135-16	135	16	A
RSSS-1-11[b]	135	11	A
RSSS-1-22[b]	135	22	A
RSSS-2-14[c]	135	14	mixture

[a] Amorphous. [b] 0.54 bmpmCl were added to this gel. [c] Gel seeded with 5 wt % of ZSM-12.

heated in air, and the temperature ramp was 20 °C/min. Chemical analyses were obtained from a Perkin-Elmer 2400 CHN analyzer. Scanning electron microscopy and EDX analyses were carried out using a JEOL JSM 6400 Philips XL30 operating at 20 kV. ^{1}H and ^{13}C NMR spectra of organic compounds were recorded on a Bruker200. Chemical shifts are quoted relative to tetramethylsilane (TMS) as an internal reference. Solid state nuclear magnetic resonance magic angle spinning (MAS) NMR spectroscopy was performed on a Bruker AV 400 spectrometer using a BL7 probe for ^{13}C and a BL2.5 probe for ^{1}F. ^{1}H to ^{13}C cross-polarization (CP) spectra were recorded using $\pi/2$ rad pulses for the proton of 4.5 μs and a recycle delay of 3 s; the samples were span at the magic angle at a rate of 5−5.5 kHz. The ^{19}F spectra were measured using pulses of 4.5 μs to flip the magnetization $\pi/2$ rad, with delays of 80 s between two consecutive pulses and spinning rates of approximately 20 kHz.

Computational Details. A computational study was carried out in order to study the most stable location of both diastereoisomers within the MTW structure. The computational methodology employed in this work is based on similar protocols that we have been recently using for studying structure directing effects in the crystallization of the FER or AFI structures.[20,22−24] The geometry of the MTW structure has been kept fixed during all the calculations. Molecular structures and the interaction energies of the organic SDAs with the framework are described with the consistent valence forcefield (CVFF);[25] this force field was originally developed for small organic molecules but has been extended for materials science applications including the simulation of zeolite and related structures, for which it has been successfully applied recently.[21−23,26,27] van der Waals and electrostatic interactions were calculated by the Ewald summation. Periodic boundary conditions (PBC) were applied in all the calculations in order to ensure the complete inclusion of SDA−SDA interactions. The atomic charges for the organic molecules were calculated by the charge-equilibration method,[28] setting the total net molecular charge to +1. In the true synthesis, the positive charge of the organic SDA molecules is compensated by the presence of the negatively charged framework (and/or fluoride ions) defects. However, because of the ill-defined nature of these defects as well as the unability of CVFF to model them, charge compensation was provided in our models by the framework by using a related version of the uniform charge background method,[29] where the atomic charge for every silicon framework atom was reduced until charge neutrality. Framework oxygen charges were kept fixed to −1.2.

The most stable location for the SDA molecules was obtained by means of simulated annealing calculations, which consisted of heating of the system from 300 to 700 K with temperature increments of 10 K and then cooling to 300 K again in the same way. A total of 500 MD steps of 1.0 fs (for a total of 0.5 ps) were run in every heating/cooling step. This cycle was repeated 10 times, and at the end of each cycle the system was geometry optimized. Then, the most stable situation was taken as representative for subsequent analysis of the location and interaction energy. The interaction energies were calculated by subtracting the energy of the molecules in vacuo to the total energy of the system.

Results and Discussion

1. Synthesis and Characterization of the Diastereoisomers. The use of the related achiral 1-benzyl-1-methyl pyrrolidinium (bmp) as SDA in pure silica preparations in fluoride medium is known to yield zeolite beta,[30] which as commented above possesses one chiral polymorph. Therefore, in an attempt to direct the crystallization of this zeolite toward the chiral polymorph A, we decided to replace bmp with a related but chiral cation, bmpm, in which the presence of two asymmetric atoms provides a chiral environment that could eventually favor the crystallization of the chiral polymorph of zeolite beta.

There are two asymmetric atoms in the bmpm molecule: one is the Cα of the pyrrolidine ring where the methanol substituent is attached, and the other one is the N atom that becomes asymmetric after the attachment of the methyl group (Figure 1). The absolute configuration of the former is certainly S in all salts, since the SDA molecule is synthesized starting from the pure chiral reactants (*S*)-(−)-*N*-benzylpyrrolidine-2-methanol or (*S*)-1-methyl-2-pyrrolidinemethanol, both with C in the S configuration (which indeed are derived from the L-proline amino acid); such an absolute configuration will remain in the final SDA product, since the organic reactions carried out in order to yield the final SDA molecule do not involve any transformation on the asymmetric C atom that is conformationally stable in proline derivatives.

Besides, if the methyl group is attached in the last step (route 1), once the benzyl group is already attached to the molecule, methylation of the N atom to produce the final

(22) Pinar, A. B.; Gómez-Hortigüela, L.; Pérez-Pariente, J. *Chem. Mater*. **2007**, *19*, 5617.
(23) García, R.; Gómez-Hortigüela, L.; Díaz, I.; Sastre, E.; Pérez-Pariente, J. *Chem. Mater*. **2008**, *20*, 1099.
(24) Gómez-Hortigüela, L.; Corà, F.; Catlow, C. R. A.; Pérez-Pariente, J. *J. Am. Chem. Soc*. **2004**, *126*, 12097.
(25) Dauger-Osguthorpe, P.; Roberts, V. A.; Osguthorpe, D. J.; Wolff, J.; Genest, M.; Hagler, A. T. *Proteins: Struct., Funct., Genet*. **1988**, *4*, 21.
(26) Moloy, E. C.; Cygan, R. T.; Bonhomme, F.; Teter, D. M.; Navrotsky, A. *Chem. Mater*. **2004**, *16*, 2121.
(27) Williams, J. J.; Smith, C. W.; Evans, K. E.; Lethbridge, Z. A. D.; Walton, R. I. *Chem. Mater*. **2007**, *19*, 2423.
(28) Rappe, A. K.; Goddard, W. A., III. *J. Phys. Chem*. **1995**, *95*, 3358.
(29) De Vita, A.; Gillan, M. J.; Lin, J. S.; Payne, M. C.; Stich, I.; Clarke, J. L. *Phys. Rev. B* **1992**, *46*, 12964.
(30) García, R.; Arranz, M.; Blasco, T.; Pérez-Pariente, J. *Microporous Mesoporous Mater*. **2008**, *114*, 312.

quaternary ammonium goes through only one side of the N atom, the opposite one to the benzyl group, due to steric reasons, thus giving place to the S absolute configuration for the N atom in the final bmpm molecule[31] (Figure 1, top). Therefore, only the S,S-bmpm diastereoisomer (hereinafter, the first letter refers to the N absolute configuration and the second one to the C absolute configuration) is obtained. However, when the quaternary ammonium cation is synthesized by benzylation of the pure chiral reactant (*S*)-(−)-*N*-methylpyrrolidine-2-methanol, due to the smaller size of the methyl substituent, the attack of benzyl chloride to the N atom can take place through both sides of the pyrrolidine ring, thus leading to a mixture of both the S,S- and the R,S-bmpm diastereoisomers (Figure 1, bottom).

The quaternary ammonium products synthesized by both routes possess CHN compositions that are close to the expected values: calculated for $C_{13}H_{20}NOI$: C = 46.8, H = 6.0, N = 4.2. Found: C = 47.1, H = 5.9, N = 4.3 and calculated for $C_{13}H_{20}NOCl$: C = 64.6, H = 8.3, N = 5.8. Found: C = 63.7, H = 8.3, N = 5.7. Figure 2 compares the ^{13}C NMR spectra of the products. In the case of the product obtained by methylation (route 1), there is only one type of carbon atom, evidencing the presence of a unique isomer, while in the spectrum of the product obtained by benzylation, there are more peaks corresponding to analogous carbons in different isomers. These results show that the product obtained by route 2 is a mixture of both the S,S and the R,S isomers. From the ^1H NMR spectra, we estimated the approximate ratio of the two isomers in this product as ∼50% (see the Supporting Information).

2. Structure Directing Effect of S,S-bmpm. *2.a. Molecular-Sieve Synthesis and Characterization.* We initially studied the structure directing effect of the pure S,S-bmpm isomer in the synthesis of all-silica zeolites in fluoride medium. Table 1 shows the synthesis conditions and the products obtained. Hereafter, the samples will be referred to with the isomer used in the synthesis, followed by the temperature and time of crystallization. The XRD patterns of the as-prepared samples indicate that this isomer efficiently directs the formation of highly crystalline ZSM-12 at temperatures of 135 and 150 °C; indeed, the zeolite is stable at both temperatures at least for as long as 25 days. It is noticeable that while the related cation bmp in similar preparations yielded zeolite beta as the only product,[30] the samples obtained with S,S-bmpm under similar conditions do not even show the presence of traces of beta at any time. Zeolite beta is considered to be a "default" phase in pure silica preparations in fluoride medium since it has been obtained with numerous SDAs.[32] However, bmpm does not yield this phase, suggesting that small changes in the molecular structure of the organic SDA have a profound effect in the products of crystallization. ZSM-12 (MTW) is a high-silica zeolite

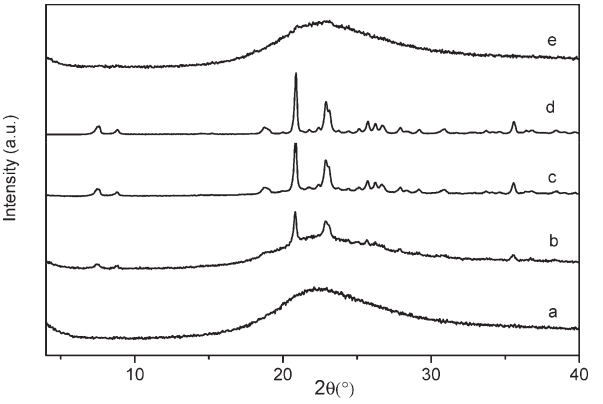

Figure 3. X-ray diffraction pattern of crystallization of ZSM-12 at 135 °C with the S,S bmpm isomer (a) 6 days, (b) 12 days, (c) 16 days, (d) 26 days, and (e) with the mixture of S,S- and R,S-bmpm isomers after 16 days of crystallization (RSSS-135-16).

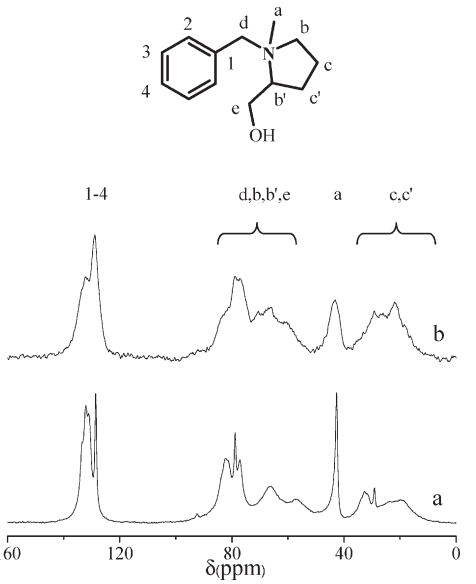

Figure 4. ^{13}C MAS NMR spectra of the (a) iodide salt of (1*S*,2*S*)-2-hydroxymethyl-1-benzyl-1-methylpyrrolidinium and (b) sample SS-135-25.

that possesses a monodimensional 12-ring channel system along the *b*-axis of the structure.[33] Indeed, beta and ZSM-12 have in common the projection of the structure along this channel, i.e., the projection of the structure of ZSM-12 along the 12-ring channel is the same as the projection along the *a* and *b* axes of the structure of zeolite beta.[34]

In order to study the kinetics of crystallization of this zeolite with the S,S-bmpm isomer, we prepared a second batch and heated the autoclaves at 135 °C for shorter crystallization times. Figure 3 shows the X-ray diffraction patterns of the products obtained after 6, 12, 16, and 26 d. We can clearly observe that zeolite ZSM-12 starts to crystallize at 12 days of heating (only amorphous material is observed in the sample heated for 6 days). After 16 days, the zeolite has crystallized almost completely, and no

(31) Dehmlow, E. V.; Klauck, R.; Düttmann, S.; Neumann, B.; Stammler, H. *Tetrahedron: Asymmetry* **1998**, *9*, 2235.
(32) Villaescusa, L. A.; Camblor, M. A. *Recent Res. Dev. Chem.* **2003**, *1*, 93.
(33) Baerlocher, C.; McCusker, L. B. Database of Zeolite Structures, **1996**, http://www.iza-structure.org/databases/.
(34) Lobo, R. F.; Zones, S. I.; Davis, M. E. *J. Inclusion Phenom. Mol. Recognit. Chem.* **1995**, *21*, 47.

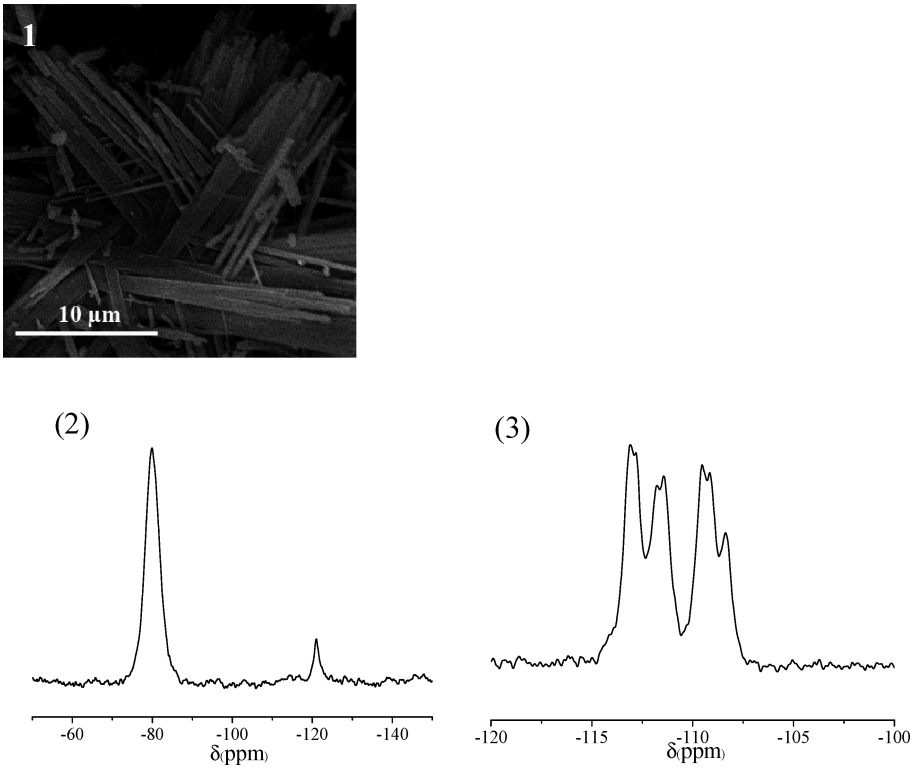

Figure 5. (1) SEM micrograph of sample SS-135-25, (2) ^{19}F MAS NMR spectrum, and (3) ^{29}Si MAS NMR spectrum of sample SS-135-25.

significant change is observed when further increasing the crystallization time.

Sample SS-135-25 was then characterized in detail by different techniques. Scanning electron microscopy (SEM) images of the sample, Figure 5-1, revealed a crystalline morphology of the samples as isolated large and well-defined needles, which is charasteristic for ZSM-12 crystals.

The organic content of the MTW sample (SS-135-25) was determined by CHN analysis. The observed C, H, and N contents were 7.83, 1.18, and 0.75%, respectively, giving a C/N ratio of 12.2, a value which is very close to that of the isolated SDA (C/N = 13), thus suggesting that the organic molecule resists the hydrothermal treatment and is indeed incorporated intact within the zeolite. The total organic content occluded in the material, estimated from the N content and taking F as the counterbalance ion, is 12% of SDAF.

The integrity of the S,S-bmpm molecule inside the zeolite framework was further assessed by ^{13}C CP MAS NMR spectroscopy. Figure 4 displays the spectrum of the iodide salt of S,S-bmpm and of the sample SS-135-25, showing the resonances corresponding to the different carbon environments in the organic molecules. All the signals of the organic cation can be distinguished in the spectrum of the zeolite, and no additional signals are observed, which confirms that the organic cation is incorporated intact within the zeolite.

Thermogravimetric analysis of sample SS-135-25 shows a gradual weight loss of 11.5% in the temperature range between 200 and 900 °C, which corresponds to the removal of the organic molecules from the inner surface of the zeolite. The absence of a noticeable weight loss below 200 °C evidences the lack of water in the sample and thus the high hydrophobicity of the material, as usually found for pure silica zeolites prepared in fluoride medium.[32] The total weight loss measured in the TGA (∼12%) is close to the amount of organic content calculated by CHN analysis and indicates that there are two molecules of bmpm per unit cell. Since the unit cell of ZSM-12 contains four channels, this indicates that the organic cation spans to two unit cells along the *b* direction, as found for other ZSM-12 materials synthesized with a related cation.[35]

The presence of fluoride in the samples was studied by ^{19}F MAS NMR (Figure 5-2). The spectrum displayed in Figure 5-2 shows a signal at a chemical shift of ∼−80 ppm, which can be assigned to fluoride within the ZSM-12 zeolite [36] and a second signal at ∼−121 ppm, which can be attributed to the presence of an impurity of SiF_6^{2-} in the sample.[37] The relative intensities of these two signals obtained by spectral deconvolution (93:7, respectively) demonstrate that the presence of the hexafluorosilicate phase is minor.

The ^{29}Si MAS NMR spectrum of the calcined material (Figure 5-3) shows several signals in the range from −107 to −117 ppm, which are assigned to $Si(OSi)_4$ (Q^4) silicate species in different crystallographic sites;[38] no signals

(35) Shantz, D. F.; Fild, C.; Koller, H.; Lobo, R. F. *J. Phys. Chem. B* **1999**, *103*, 10858.
(36) Koller, H.; Wölker, A.; Villaescusa, L. A.; Díaz-Cabañas, M. J.; Valencia, S.; Camblor, M. A. *J. Am. Chem. Soc.* **1999**, *121*, 3368.
(37) Camblor, M. A.; Barrett, P. A.; Diaz-Cabanas, M.-J.; Villaescusa, L. A.; Puche, M.; Boix, T.; Perez, E.; Koller, H. *Microporous Mesoporous Mater.* **2001**, *48*, 11.
(38) Fyfe, C. A.; Gies, H.; Kokotailo, G. T.; Marler, B.; Cox, D. E. *J. Phys. Chem.* **1990**, *94*, 3718.

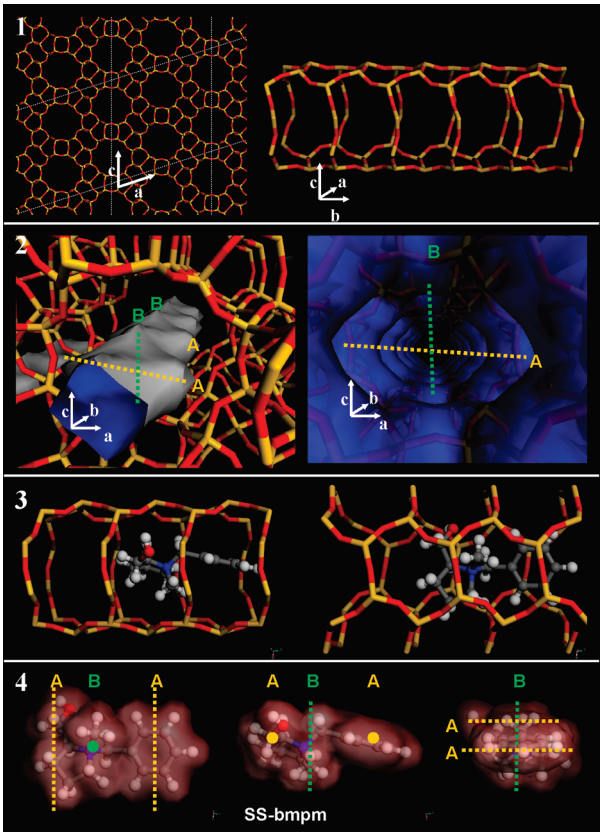

Figure 6. (1, left) Projection of the MTW structure and (right) channel walls. (2) MTW channel structure, showing the free volume (left) and the VdW surface (right), highlighting the side-cavities. (3) Two views of the most stable location of S,S-bmpm (position 1) inside the MTW channel. (4) Structural relationship between the S,S-bmpm isomer and MTW (2).

associated with connectivity defects are observed, as usually found in samples obtained in fluoride medium since the charge of the organic cations is compensated by fluoride rather than by negatively charged connectivity defects. The overall spectrum displays three broad signals, three of which are in turn split into two signals, in agreement with the seven independent T-sites of the asymmetric unit of the MTW structure.[38]

2.b. Computational Study. The experimental results previously presented demonstrate that the S,S-bmpm isomer directs the crystallization of ZSM-12 instead of the zeolite beta. In this section we try to understand the structure directing efficiency of this SDA with the aid of computational simulation techniques.

Figure 6 shows a projection of the MTW structure (1), the channel walls and two different views of the MTW channel system (2); one with the van der Waals surface (right) and the other one showing the free volume inside the channel (left). The 12 MR channels are one-dimensional, elliptical, and not interconnected. The channel walls are formed by 6 MR and 10 MRs which form side-cavities.

2.b.1. Location of S,S-bmpm along the MTW Channel. In order to understand the structure directing effect of the bmpm molecule in the synthesis of ZSM-12, first we studied the location and interaction energies of the SDA molecule by docking one single S,S-bmpm molecule within the 12 MR channels of the MTW structure. For this set of calculations, one S,S-bmpm molecule was loaded in a $1 \times 1 \times 4$ MTW supercell. There are two possible orientations for the bmpm molecules within the MTW channels, which are related by rotating the pyrrolidine ring around the $N-CH_2$ bond, whose respective interaction energies with the MTW framework are -134.5 and -108.6 kcal/mol per S,S-bmpm molecule, respectively, evidencing that the occluded molecules will only orient as the former. Figure 6-3 shows the most stable orientation of the molecule, where the pyrrolidine ring is roughly aligned with the channel direction, with the most outermost group, which is the methanol substituent, pointing toward the larger 10-ring side-cavities of the channel. The two bmpm molecular rings, the pyrrolidine and the phenyl rings, are oriented with the ring axis parallel to the larger cross section of the elliptical channel, this is, parallel to "a".

We then studied the energy diagram for the location of the molecule in different positions along the channel axis, searching for stable positions along the channel. The molecules were manually displaced along the *c* axis by 1 Å steps and then geometry optimized. Only two stable positions were identified (positions 1 and 2): all the different molecular locations along the 12 MR channel direction reverted to one of these two positions. Position 1 is clearly more stable than position 2, with the energy difference around 12 kcal/mol, due to a better fitting of the molecular groups with the channel topology (Figure 6-3). The high energy difference evidences that the S,S-bmpm molecule will be occluded in the MTW structure during the synthesis mostly in position 1. These energy results demonstrate the existence of one preferred well-defined site along the channel axis for accommodating the S,S-bmpm molecule, where the methanol substituent and the benzyl rings are pointing toward the side cavities while the methyl group is pointing toward the center of a six-ring (Figure 6-3).

A detailed analysis of the molecular structure of S,S-bmpm and of the MTW void volume available revealed a clear structural relationship between them, as shown in Figure 6, which explains the high efficiency of this molecule in directing the MTW synthesis. There are two types of side pockects along the MTW channel: one delimited by 10-rings, which are on opposite sides in the "a" direction (referred to as A cavities in Figure 6-2), and other two delimited by 6-rings, on opposite sides of the "c" direction (referred to as B), smaller than the previous; both types of cavities are arranged perpendicularly and alternatively (B−A−B). Meanwhile, a related molecular structure can be found in the S,S-bmpm molecule: there are two longer molecular axis parallel to "b", one corresponding to the axis crossing the pyrrolidine ring with the methanol subsituent and the other through the benzyl ring (these are referred to as A in Figure 6-4); these axes will align within the A cavities in MTW due to their larger cross-section. In addition, we can define another perpendicular molecular axis, though of a lower length, perpendicular to the previous ones, going through the methyl

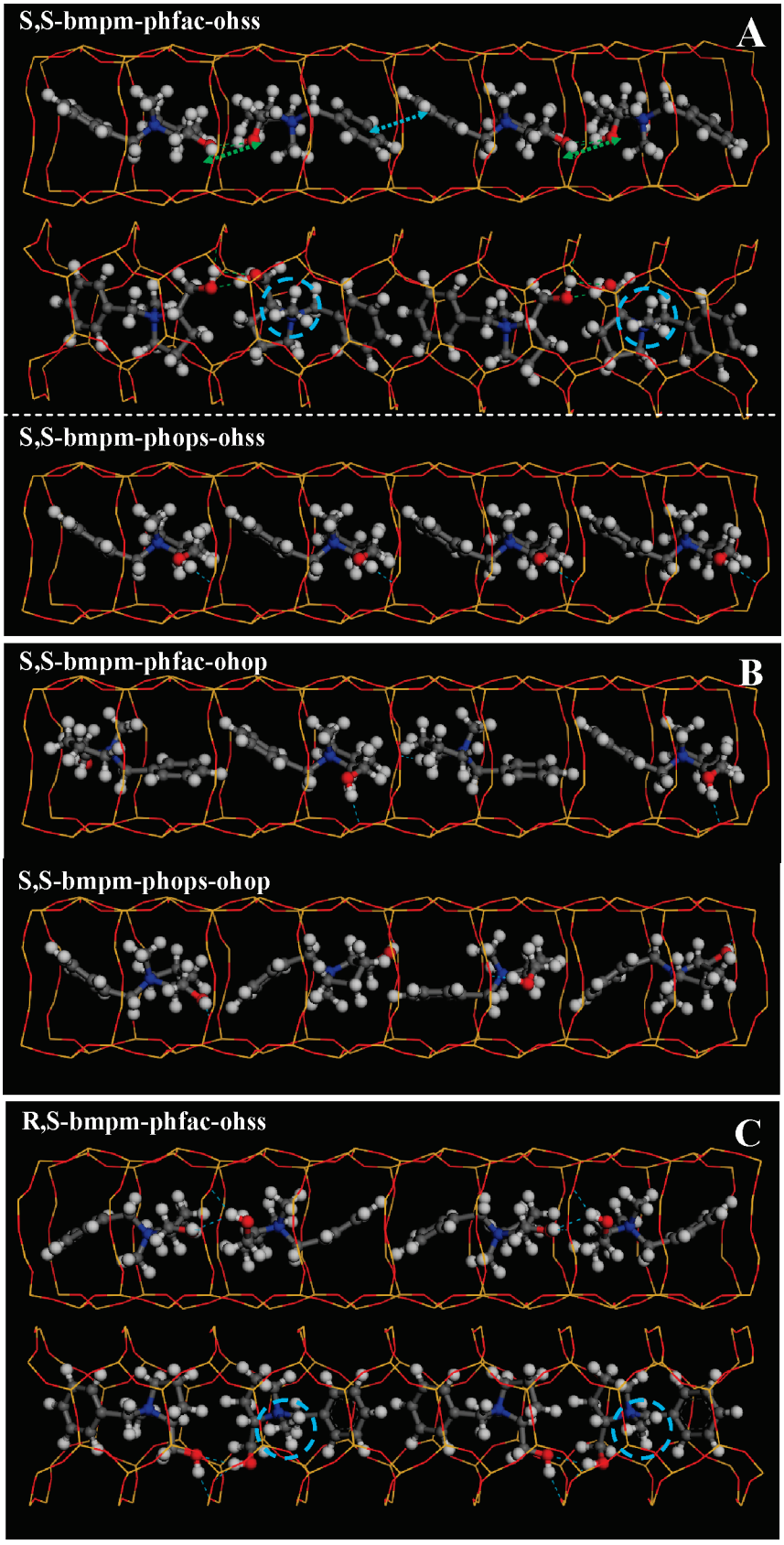

Figure 7. Location of S,S-bmpm molecules in the different orientations, with methanol groups oriented toward the same side and phenyl rings facing each other (phfac-ohss, A-top, two views are shown) or benzyl rings in opposite sides (phopp-ohss, A-bottom), with methanol in opposite sides and benzyl rings facing each other (phfac-ohop, B-top) or benzyl rings in opposite sides (phopp-ohop, B-bottom). (C) Two views of the most stable location of R,S-bmpm isomers, with methanol groups in the same side and benzyl rings facing each other (phfac-ohss). Dashed green lines indicate H-bonds, while dashed circles highlight the fitting of methyl groups with the six rings; dashed green and blue arrows indicate the intermolecular interactions between S,S-bmpm (H-bonds and π π-type, respectively) that gives place to a chain molecular arrangement.

and methylene groups (referred as B) that will locate in the smaller B-type cavities of the structure. Such A and B molecular axes are also arranged perpendicularly and alternatively (B−A−B) and with a similar distance between them as in the MTW structure. Therefore, this close structural relationship between the molecular structure of S,S-bmpm and the MTW topology explains the high ability of this molecule to direct the synthesis of this framework.

2.b.2. Packing of S,S-bmpm. Once understood the preferential siting of the S,S-bmpm isomers in the channel, we studied the packing between consecutive S,S-bmpm molecules. Because of the noninterconnection between different channels, molecules sited in different MTW channels will not interact among each other; hence, only molecules in one channel have been studied. Four molecules were initially loaded in a single channel in a $1 \times 1 \times 8$ MTW supercell. This gives an organic content of two molecules per unit cell, which is in good agreement with the experimental value. The obtained energies were then multiplied by 4 (since there are 4 channels per unit cell) and normalized to one unit cell. Consecutive bmpm molecules can be packed in different relative orientations: with phenyl rings of consecutive molecules facing each other ("phfac") or in opposite sides ("phopp"). In addition, methanol substituents of consecutive molecules can be oriented in the same side ("ohss") or in opposite sides ("ohopp"). Overall, four different relative orientations of the molecules were studied by means of simulated annealing calculations.

The most stable location of the molecules is shown in Figure 7. The associated interaction energies for these orientations were calculated as −245.3 and −237.6 kcal/mol for phfac-ohss and phfac-ohopp orientations, and −241.1 and −233.0 kcal/mol for phopp-ohss and phopp-ohopp orientations, respectively. These energy results show that the orientation where the methanol groups of consecutive molecules are in the same side is more stable than when they are pointing in opposite directions, regardless of the relative orientation of the aromatic rings. This might be due to a better fitting between consecutive rings (benzyl−benzyl in "phfac" or benzyl−pyrrolidine in "phopp" orientations) and also to a better adjustment with the channel topology (with the side pockets). In addition, the orientation with benzyl rings facing each other is more stable (by ∼4 kcal/mol per MTW unit cell (u.c.)). Overall, the most stable orientation hence is with benzyl rings facing each other and methanol groups pointing toward the same side (Figure 7-A, top).

The higher stability of this organic arrangement (S,S-bmpm-phfac-ohss) is due to, first, a good fitting between the molecular arrangement and the channel topology in terms of the structural relationship as previously commented (Figure 6); second, to a stabilizing interaction between consecutive aromatic rings through $\pi-\pi$ interactions, and finally, to the development of a double H-bond between the methanol groups of consecutive molecules. These two types of interactions between consecutive molecules, $\pi-\pi$ type interactions between aromatic rings, and double H-bonds between methanol groups, generate a molecular chain arrangement of self-assembled S,S-bmpm molecules along the MTW channel, which is detailed in Figure 7A-top. It is worth noting that in this most stable orientation, the methanol groups are always located in the same side all along each 12MR channel, thus generating an asymmetric environment in the channels.

A higher packing value of 2.5 molecules per unit cell was also tried. In this case, the only possible molecular orientation able to reach such a high packing value is with benzyl rings facing each other and methanol groups oriented toward the same side. The interaction energy developed under this molecular arrangement was −174.9 kcal/mol per MTW u.c., evidencing a high unstability for this packing value compared to the previous interaction energy (under a packing of 2 molecules per u.c., ∼−245 kcal/mol), thus evidencing that the most stable molecular packing is of 2 molecules per unit cell, in agreement with the experimental observations.

3. Structure Directing Effect of R,S-bmpm. So far, the experimental and computational results have demonstrated the existence of a true templating effect of the S,S-bmpm molecule when directing the synthesis of the MTW structure due to a close structural complementary relationship between the molecular and the channel structures. Such strong templating effect led us to wonder if a subtle modification of the molecular geometry such as the inversion of the absolute configuration of the N atom, giving place to the R,S-bmpm diasteroisomer, could have an important influence over the structure directing ability of this molecule. We then first studied computationally the interaction energy of this new isomer with the MTW structure and then tried to experimentally validate the observations of the simulation study.

3.a. Computational Study. 3.a.1. Interaction of R,S-bmpm with the MTW Structure. The same set of calculations as in the previous sections (with S,S-bmpm) have been performed for the R,S-bmpm isomer. When studying one molecule in a $1 \times 1 \times 4$ u. c. MTW, i. e., without considering packing effects, we observed that again the most stable orientation was the same as for the previous diasteroisomer, developing an interaction energy with the framework of −132.5 kcal/mol per molecule. Interestingly, this interaction energy of one single molecule of the R,S-diasteroisomer is slightly lower than that of the S,S (R,S, −132.5 kcal/mol; S,S, −134.5 kcal/mol).

When packing effects were considered (four molecules in the same channel in a $1 \times 1 \times 4$ u.c. MTW supercell), the interaction energy was calculated as −233.2 kcal/mol per MTW u.c. in the most stable configuration (same orientation as S,S, with benzyl rings facing each other and methanol groups oriented in the same side, phfac-ohss). This energy is much lower than the corresponding for S,S (−245.3 kcal/mol per MTW u.c.), suggesting a more efficient structure directing ability of the S,S diasteroisomer for the synthesis of the MTW structure. The most stable location of the R,S-bmpm molecules is shown in Figure 7C. The lower interaction of the R,S-bmpm isomer

with the MTW structure is due to a worse fitting of the R,S molecular geometry within the channel topology; if we compare with the location of S,S-bmpm, we can observe that the fitting of the methyl groups with the 6-rings of the channel is better in the S,S isomer, where they point to the center of the ring, than in the R,S one, where they are bent, as highlighted in parts A and C of Figure 7 by dashed circles; this is due to the different relative configuration of the methyl and methanol substituents, which are in syn (in the same side) or anti (opposite sides) configurations in S,S and R,S isomers, respectively (see Figure 1-right). Besides, the lower interaction of R,S-bmpm might also be due to a less effective packing of these isomers along the channel, since in this case only one H-bond is developed between consecutive molecules, in contrast to the double H-bond observed for the S,S isomer.

3.a.2. Interaction of an Equimolar Mixture of S,S- and R,S-bmpm with MTW. Our simulation study thus suggests a much lower structure directing efficiency of the R,S isomer in the synthesis of the MTW structure; we now attempted to experimentally validate this theoretical observation. However, as commented in the introduction, only an equimolar mixture of both diasteroisomers rather than the isolated R,S isomer is obtained by direct synthesis following the approach described here. Hence, we finally simulated the interaction of an equimolar mixture of diasteroisomers by the same computational methodology. The two diasteroisomers were arranged alternatively (note: other arrangements were tried but lower interaction energies were found). The most stable orientation involved the molecules with benzyl rings facing each other but due to the different absolute configuration of consecutive molecules, in this case, methanol subsituents were located in opposite sides, hence letting the aromatic rings of consecutive molecules to arrange parallel to each other, developing strong $\pi-\pi$ type interactions. The interaction energy observed for this system was −240.9 kcal/mol per MTW u.c., which is in between that for the pure systems (S,S, −245.3 kcal/mol; R,S: −233.2 kcal/mol). Therefore, these results also suggest a lower efficiency of the mixture of isomers to direct the crystallization of the MTW structure.

3.b. Molecular-Sieve Synthesis. Finally, we performed a set of zeolite synthesis experiments by using the mixture of diastereoisomers (R,S) and (S,S) bmpm (RSSS-135, Table 1). The experiments were performed with a similar gel composition and at 13 and 16 days where the crystallization of ZSM-12 with the pure S,S-bmpm isomer had already finished. The XRD patterns of the new samples (Figure 3) clearly show that when the mixture of isomers is employed in the synthesis of ZSM-12, a dramatic effect over the crystallization of the ZSM-12 zeolite is observed. An amorphous material is obtained with the mixture of isomers after 13 days of crystallization, while ZSM-12 had already started to crystallize after 12 days when the S,S isolated isomer was used as the SDA. In addition, while after 16 days the S,S isomer yields well-crystallized ZSM-12, the sample obtained with the mixture of isomers is still mostly amorphous. Therefore these results evidence that the mixture of isomers, and so the R,S isomer, is not able to direct the crystallization of ZSM-12, in contrast to the S,S isomer itself, in good agreement with the predictions suggested by the computational study.

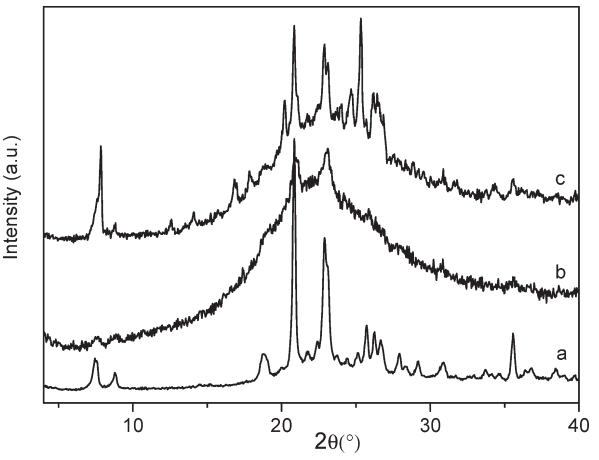

Figure 8. X-ray diffraction pattern of (a) ZSM-12 synthesized with the S,S-bmpm isomer at 16 days (sample SS-135-16), (b) physical mixture of ZSM-12 (5 wt %) in amorphous silica, and (c) sample RSSS-2-14.

The lower efficiency of the structure directing ability of the mixture of isomers might be due either to the incorporation of the two isomers within the MTW structure during crystallization, with the consequent decrease of the interaction with the framework due to the occlusion of R,S-bmpm, to the lowering of the concentration of the S,S isomer in the synthesis gel, or to the combination of both factors together.

In order to answer the above questions, we performed subsequent experiments (RSSS-1-and RSSS-2, Table 1). In one of them, we increased the total organic content in the synthesis gel to 1.08 by adding 0.54 mol of the chloride salt of the mixture of bmpm isomers, so that the total content of 1S,2S was equivalent to that in the pure form that leads to ZSM-12. The resulting product was an amorphous material even at long crystallization times (22 days), therefore suggesting that the presence of the 1R,2S impedes the nucleation of ZSM-12. In a second experiment (RSSS-2-14), the gel with the mixture of isomers was seeded with a small amount of ZSM-12 (∼5 wt % of zeolite). In this case, the XRD pattern of the product (Figure 8) showed the crystallization of a mixture of phases, though some diffractions of ZSM-12 can be identified. Comparing the intensity of these diffraction peaks with those of a 5 wt % physical mixture of zeolite ZSM-12 and amorphous silica indicates that there has been some crystalline growth. Therefore, the above results suggests that the low structure directing ability of the mixture of isomers is due to a blocking of the ZSM-12 nucleation provoked by the presence of 1R,2S-bmpm molecules, which compete to be incorporated within the nascent MTW structure, thus preventing further growth of the zeolite. The effect of the (1R,2S) isomer is mainly exerted over the nucleation of ZSM-12 rather than over crystal growth, though both are disfavored.

The fact that such a subtle change in the molecular structure of the SDA molecule can dramatically alter the structure directing ability of a molecule suggests that the S,S-bmpm plays a true templating effect in the synthesis of this zeolite, as previously mentioned.

Our results opens up a new possible application of zeolites in enantioselective/diasteroselective processes. Indeed, the diasteroespecificity in the synthesis of zeolite structures by using chiral SDA molecules, as the example studied in this work, could eventually be used as a diasteroselective separation process, in which the preferential structure directing ability of one of the diastereoisomers would lead to a partial enrichment of the zeolite in a specific diasteroisomer (and the opposite in the mother liquors), provided the other isomer does not have a blocking effect on the zeolite crystallization, as occurred in the present case.

Conclusions

This work describes experimental and theoretical studies about the structure directing efficiency of two diastereoisomers [(1*S*,2*S*) and (1*R*,2*S*)] of the cation 2-hydroxymethyl-1-benzyl-1-methylpyrrolidinium in the synthesis of pure silica zeolites in fluoride medium. Experimental results indicate that the 1S,2S diastereoisomer directs very efficiently the crystallization of ZSM-12. Such a highly efficient structure directing role of this isomer is due to a close structural relationship between the SDA and the framework, whose molecular geometries are indeed complementary. Interestingly, the most stable arrangement of these isomers within the MTW channels involves the development of a molecular chain where the SDAs are self-assembled through $\pi-\pi$ type interactions between the aromatic rings and double H-bonds between methanol attached to pyrrolidine groups, thus generating a chiral molecular arrangement which efficiently stabilizes the MTW structure by developing strong nonbonded interactions. However, experiments trying to synthesize the same zeolite with a ~1:1 mixture of the 1S,2S and 1R,2S isomers failed in producing crystalline ZSM-12, which is explained by the low interaction that the latter isomer develops with the MTW framework, thus blocking the structure directing effect of the efficient SS-isomer. Therefore, our results provide a new example of a true templating effect, which in turn is diasterospecific, observed in the synthesis of zeolite materials.

Acknowledgment. We are thankful for the financial support of the Spanish Ministry of Science and Innovation (MICINN, former MEC), Projects CTQ2006-06282 and MAT2006-14274-C02-02. R. García acknowledges CSIC for a JAE contract. L. Gómez-Hortigüela is grateful to the Spanish Ministry of Science and Innovation for a postdoctoral fellowship. We thank Accelrys for providing their software and Centro Técnico de Informática for running the calculations.

Supporting Information Available: ^{1}H NMR spectra of the organic salts of the pure 1S,2S-bmpm isomer and of the mixture of the 1S,2S and 1R,2S-bmpm isomers (PDF). This material is available free of charge via the Internet at http://pubs.acs.org.